Available online at www.sciencedirect.com
ScienceDirect
Polymer Degradation and Stability 93 (2008) 889–895
Polymer Degradation and Stability
www.elsevier.com/locate/polydegstab

In situ polymerized poly(butylene succinate)/silica nanocomposites: Physical properties and biodegradation

Sang-Il Han [a], Jung Seop Lim [d], Dong Kook Kim [b], Mal Nam Kim [c], Seung Soon Im [d,*]

[a] *Material Lab, Corporate R&D Center, Samsung SDI Co., Ltd., 575, Shin-dong, Yeongtong-gu, Suwon-si, Gyeonggido 443-391, South Korea*
[b] *Department of Chemistry, Hanyang University, Ansan, South Korea*
[c] *Department of Biology, Sangmyung University, 7 Hongji-dong, Chongro-gu, Seoul 110-743, South Korea*
[d] *Department of Fiber and Polymer Engineering, Hanyang University, Haengdang-dong, Seongdong-ku, Seoul 133-791, South Korea*

Received 26 November 2007; received in revised form 12 February 2008; accepted 20 February 2008
Available online 29 February 2008

Abstract

A series of poly(butylene succinate)/silica (PBS/silica) nanocomposites were prepared by *in situ* polymerization. Solid-state ^{29}Si NMR and FTIR analysis indicated that silanol-bonded carbonyl groups are established within PBS/silica nanocomposite materials. Rheological effects inherent to the silica filler were evaluated by melt rheological analysis as a function of shear force in the molten state. Despite high shear force, PBS/silica nanocomposites maintained a relatively high melt viscosity, attributable to a network structure resulting from covalent bonding between silica and the polymer chain. Nanocomposite material containing 3.5 wt% silica exhibited greatly improved mechanical properties. The tensile strength at break and elongation were *ca*. 38.6 MPa and 515%, while those of the parent PBS were 26.3 MPa and 96%, respectively. PBS/silica nanocomposites showed composition dependency on biodegradation ascribable to reduced crystallinity and preferential microbial attack.

Keywords: Poly(butylene succinate); Silica; Nanocomposite; Biodegradation

1. Introduction

Nowadays, PBS-based polymers have attracted a great deal of interest as promising biodegradable materials. Among the manufacturing methods available for PBS-based polymers, copolymerization and blending have proven to be effective with regard to improvement of the mechanical properties and biodegradability [1–6]. However, these methods often give rise to problems affecting the physicochemical properties of the polymer. Incorporation of a secondary component above 20 mol% reduces the crystallinity of the parent polymer and significantly reduces the melting point due to imperfect lateral packing and/or isomorphism, and adversely affects the temperature range over which they can be used [7–9].

Another manufacturing method for biodegradable PBS-based polymers is as a nanocomposite with an inorganic material, such as silica or clay, acting as a structural reinforcement. However, the inorganic components tend to aggregate when processed into a nanocomposite due to strong hydrophilic interactions. Therefore, a number of studies of biodegradable polymer/inorganic composites have focused mainly on the dispersibility of inorganic materials within the polymer matrix and the resulting physical properties [10–12]. Recently, using small-angle X-ray scattering (SAXS) and transmission electron microscopy (TEM), Kim et al. [13] investigated the thermal stability of a PBS/organoclay composite and demonstrated that a chemical reaction between the epoxy groups of the organoclay and the end groups of PBS improved the thermal stability of the composite. Lim et al. [14] manufactured a poly(3-hydroxybutyrate-*co*-3-hydroxyhexanoate) (PHB–HHx)/silica composite using simple melt compounding and found that the formation of intermolecular hydrogen bonds between PHB–HHx and silica slowed the rate of crystallization.

Despite these studies, little is known about the physical properties and biodegradation of *in situ* polymerized PBS/silica

* Corresponding author.
E-mail address: imss007@hanyang.ac.kr (S.S. Im).

0141-3910/$ - see front matter © 2008 Elsevier Ltd. All rights reserved.
doi:10.1016/j.polymdegradstab.2008.02.007

composite. The present study was performed to investigate the chemical structure of PBS/silica composites prepared by *in situ* polymerization. Melt rheological properties and biodegradability were evaluated during biodegradation in compost.

2. Experimental

2.1. Materials and polymerization

Succinic acid, 1,4-butanediol, titanium tetrabutoxide, and fumed silica (Aerosil R300) were obtained from Aldrich (St. Louis, MO) and used without further purification. PBS/silica composites were prepared in the presence of fumed silica (~5.5 wt% of total monomer) by *in situ* two-step polymerization consisting of direct esterification and polycondensation. Slurry composed of succinic acid, 1,4-butanediol, and fumed silica was prepared in a reactor equipped with an overhead stirrer and a temperature controller. A flask containing succinic acid and 1,4-butanediol (1:1.2 by mole ratio) was heated to 190 °C in an oil bath with mechanical stirring at 300 rpm. The fumed silica was then added under a nitrogen atmosphere. The resulting monomer mixture was melted and stirred at 190 °C for 2 h, evolving water condensate. The reaction temperature was then raised to 240 °C over a period of 30 min, with gradual application of reduced pressure to remove low molecular weight condensates, and maintained at 240 °C for 3–5 h depending on the feed composition. The resulting poly(butylene succinate)/silica composites are denoted as follows: e.g., PBS/silica-1.8 represents poly(butylene succinate) containing 1.8 wt% silica.

2.2. Solid-state ^{29}Si NMR spectroscopy and polymer characterization

Solid-state ^{29}Si NMR spectra were recorded using a 200 MHz spectrometer (Unity Inova 200; Varian, Palo Alto, CA). These spectra yield quantitative information about Si atom coordination or substitution around reacted $R'_nSi(OR)_{4-n}$ units, where $n = 1$, 2, or 3. For a tetrafunctional silicate with SiO_4 tetrahedral subgroups, five Q peaks (Q_0, Q_1, Q_2, Q_3, Q_4) are present in the NMR spectra. Inherent viscosity was determined using a Cannon-Ubbelohde microviscometer at a concentration of 0.3 g dL^{-1} in chloroform at 25 ± 0.1 °C. Samples for DSC, DMA, WAXD, and tensile testing were prepared on a compress mold machine. The temperature was set 30–50 °C above T_m. After melting, samples were quenched in ice water. Before use, all samples were dried in a vacuum oven at 40 °C for 48 h. The thermal properties of PBS and PBS/silica nanocomposites were analyzed using a Perkin Elmer DSC-7 differential scanning calorimeter. Upon melting, the samples were heated to 160 °C at a rate of 10 °C/min. The apex of the melting peak was taken as the melting temperature. The loss modulus was measured as a function of temperature by dynamic mechanical analysis (TA-DMA 2980) at a frequency of 1 Hz under a nitrogen atmosphere. Samples were quenched to −100 °C and then heated gradually to 130 °C at a rate of 2 °C/min. The peak position of loss modulus was taken as the glass transition temperature.

2.3. Melt rheological analysis

The rheological properties of the nanocomposites in the molten state were measured at 150 °C using a dynamic oscillatory rheometer (ARES; Rheometric Scientific Inc., Piscataway, NJ) equipped with parallel plates with a diameter of 20 mm and a gap of 1.0 mm. The frequency ranged from 0.1 to 400 rad/s. Rheological specimens were dried for 24 h in a vacuum oven at 60 °C prior to measurements.

2.4. Stress–strain measurements

Mechanical properties were measured on a TA 4465 instrument with a 1 kN load cell and a grip distance of 26 mm at a cross-head speed of 10 mm/min. Polymer films were prepared on a dumbbell-shaped film with the following dimensions: 3.5 mm (width), 14 mm (gage length), and 0.3 mm (thickness).

2.5. Wide angle X-ray diffraction (WAXD) and transmission electron microscopy (TEM)

Micro-structural changes in the nanocomposite materials were investigated by wide angle X-ray diffraction (WAXD) using an X-ray diffractometer equipped with a nickel-filtered Cu Kα source (40 kV, 30 mA, Model DMAX 2000; Rigaku Denki, Tokyo, Japan). Spectra were obtained at room temperature at a scan speed of 10°/min over a range of 5–40°. The interfacial surface morphology was examined by transmission electron microscopy (TEM) using a JEOL 2000EX(II) (JEOL Ltd., Tokyo, Japan). Samples for TEM analysis consisted of ultra-thin sections ranging from 40 to 60 nm in thickness prepared with a diamond knife at a temperature of −40 °C on a Reichert–Jung Ultracut microtome (Leica, Wetzlar, Germany).

2.6. Preparation of the mature compost

Animal fodder (Samyant Oil & Feed Corporation, Incheon, Korea) was used as the compost substrate. The composition of fiber, fat, and protein in this mixture was similar to human food garbage. Composting was performed at a maximum temperature of 58 °C during the thermophilic phase with the moisture content maintained at 65%. The composting process lasted for 50–60 days.

2.7. Evaluation of biodegradability in the mature compost

All specimens for biodegradation testing were cryogenically ground into a powder (particle size: *ca.* 80 μm) and dried to a constant weight. Biodegradation of the nanocomposites was conducted in the laboratory-scale compost described above according to ASTM D5209-92 (1992) and ASTM D5338-92 (1992). Airflow was maintained at 40 mL/min. A mixture of

mature compost (wet weight: 200 g) and nanocomposite material (5% on a dry basis) was incubated at 58 °C. Carbon dioxide produced from the compost was absorbed by a solution of 0.4 N potassium hydroxide and 2 N barium chloride and quantified by titrating the solution with 0.2 N HCl.

3. Results and discussion

Fig. 1 shows representative results of solid-state ^{29}Si NMR of PBS/silica-3.5, providing information regarding Si atom coordination. The spectral data related to Q peaks were as follows: Q0: −72 to −82 ppm, Q1: −82 to −89 ppm, Q2: −92 to −96 ppm, Q3: −100 to −104 ppm and Q4: ∼ −110 ppm [15–18]. The shoulder at −106.8 ppm indicates covalent bonding between Si and the PBS polymer backbone chain.

Additional proof for this covalent bonding state was provided by the FTIR spectrum shown in Fig. 2, at which pure PBS exhibited the characteristic carbonyl bands at 1723 cm^{-1}. Interestingly, as for PBS/silica-1.8, a small shoulder-like band may be assigned around 1717 cm^{-1}. Furthermore, the intensity of this band became developing in proportion to the added silica content. On the whole, if specific intermolecular interaction is formed between the carbonyl group of polyester and the functional group of other materials, some modification near this carbonyl group can be detected. For example, the wavenumbers of carbonyl group may be shifted [14,19], or new carbonyl groups near the major carbonyl group can be created [20,21]. Based on this, this new peak at 1717 cm^{-1} can be considered to be a result of the interaction between the silanol group and carbonyl groups and the strength of this intermolecular bonding became more powerful with the increases of silica contents. A similar result was reported in the work of Lim et al., who showed that the carbonyl group of PBS molecules interacted with the −NHCO− groups of urethane between silica particles and PBS molecules, giving rise to the formation of intermolecular interaction in PBS/isocyanate-modified silica nanocomposites [22].

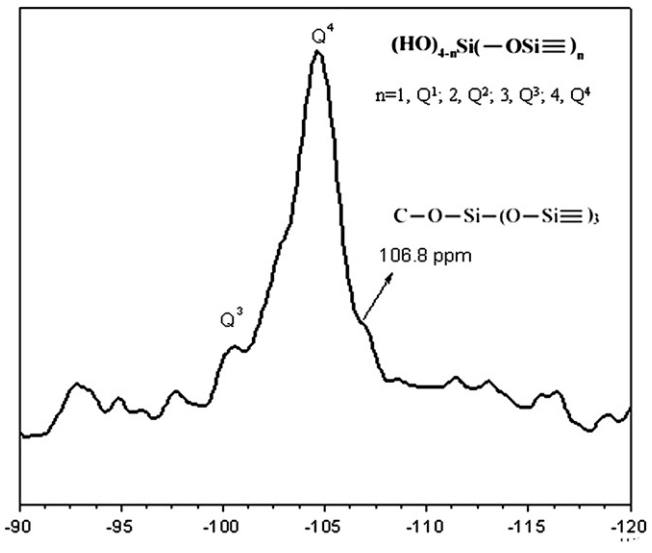

Fig. 1. Solid-state ^{29}Si NMR spectra for PBS/silica-3.5.

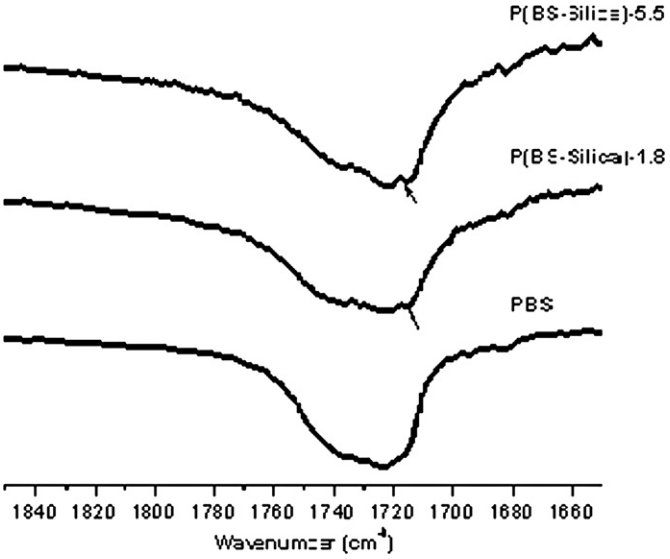

Fig. 2. FTIR spectra for PBS/silica nanocomposites.

Table 1 summarizes the physical characteristics of PBS and PBS/silica nanocomposite materials. The inherent viscosity (η_{inh}) of PBS/silica nanocomposites ranges between 0.71 and 1.28 dL g^{-1}. Consistent increases in η_{inh} were observed with the incorporation of ∼3.5 wt% silica. Conversely, a silica content of 5.5 wt% or higher markedly decreased η_{inh}. These results may reflect increased reactivity of polyester in the presence of fumed silica during the polycondensation process [23,24]. Consequently, these results suggested that 3.5 wt% of silica leads to an increase in the degree of polymerization in the PBS/silica nanocomposite by acting as a catalyst during the polymerization process. PBS/silica-1.8 and 3.5 showed slight increases in glass transition temperature with increasing silica content without significant changes in the melting temperature. The crystallinity of the parent PBS was 52.5%, while the values for nanocomposites were significantly lower. In the case of PBS/silica-3.5, the crystallinity was 36.2%; a decrease of about 38.7% from that of the parent PBS. WAXD patterns of all specimens exhibited distinct crystalline reflections of the (020), (021), (110), and (111) planes ($2\theta = 19$, 21.5, 22.5, and 28°, respectively) (data not shown). As silica content increased, WAXD curves broadened without any further significant changes.

The loss tangent (tan δ) curves for parent PBS and PBS/silica nanocomposites prepared via *in situ* polymerization in the molten state are shown in Fig. 3(a). Tan δ is generally measured as an indicator of the solid-like elastic or liquid-like viscous properties of a system. The tan δ curves of PBS/silica-1.8 and PBS/silica-3.5 showed broader peaks with higher intensity than the parent PBS due to significant phase segregation in the nanocomposite system. This behavior is detailed in the Cole–Cole plots shown in Fig. 3(b). While the slope of the parent PBS was approximately 2.0 over all frequencies, the slopes of PBS/silica-1.8 and 3.5 were 0.97 and 0.73, respectively. Another conspicuous observation was that inflection points appear on the Cole–Cole plots in the vicinity of $G'' = 2390$ Pa. Based on the report by Han et al. [3] indicating

Table 1
Polymer characterization of PBS and PBS/silica nanocomposites

Sample code	Silica content (wt%)[a]	η_{inh}[b] (dL g^{-1})	T_g[c] (°C)	T_m[d] (°C)	ΔH_f (J/g)	X_c[e] (%)
PBS	0	1.18	−10.9	115.4	80.6	52.5
PBS/silica-1.8	1.8	1.20	−9.1	114.6	70.3	35.4
PBS/silica-3.5	3.5	1.28	−9.2	114.6	70.4	36.2
PBS/silica-5.5	5.5	0.71	–	115.4	82.3	–

T_g and X_c of PBS/silica-5.5 could not be measured because compress molded film was extremely brittle.

[a] Weight ratio of silica to total monomer in feed.

[b] At 25 °C, 0.3 g dL^{-1} in chloroform solution.

[c] Measured by DMA, 5 °C/min.

[d] Measured by DSC, 10 °C/min.

[e] Calculated by deconvolution of the WAXD patterns using curve-fitting profram.

that a slope approaching 2.0 corresponds to an isotropic and homogeneous system, the PBS/silica nanocomposites were thought to behave as heterogeneous systems below critical shear force. This may be attributed to the existence of a network structure originating from interactions between silica particles, or from interactions between silica particles and polymer chains. With increasing shear force, the network structure is broken and thus the PBS/silica nanocomposite material appears to approach a homogeneous state. In addition, the viscosity curve in Fig. 3(c) shows that the PBS/silica nanocomposites exhibited higher viscosity than the parent PBS polymer at all frequencies examined, probably due to the filler effect of silica particles on the PBS matrix. In contrast, the melt viscosity of PBS/silica nanocomposites decreased slightly with increasing frequency, while the parent PBS maintained a nearly constant melt viscosity irrespective of increasing frequency. In our previous study [23] of the melt rheological properties of PET/silica nanocomposites,

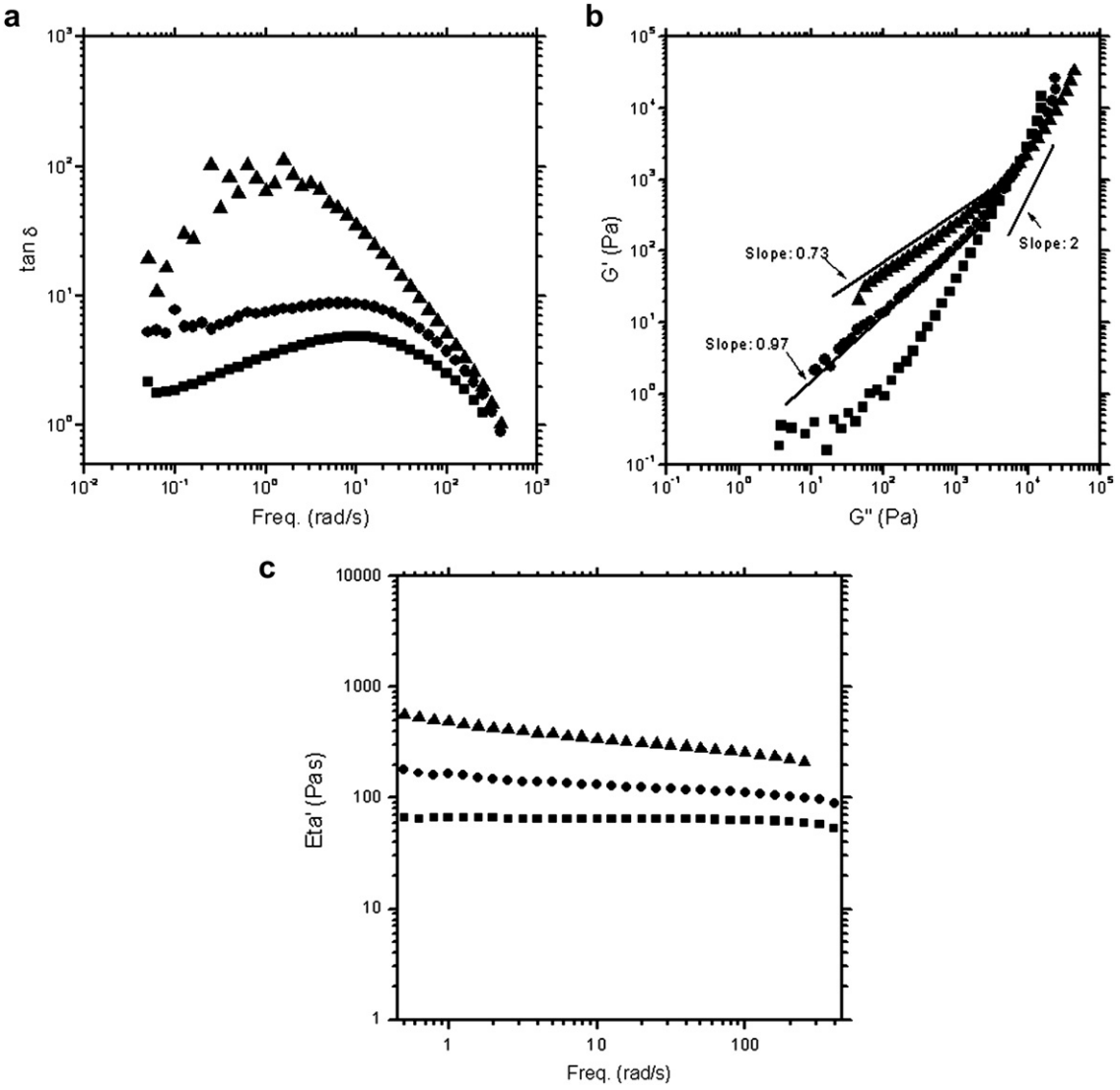

Fig. 3. Variation of (a) tan δ, (b) Cole–Cole plot, and (c) viscosity of PBS/silica nanocomposites as a function of frequency at 150 °C. PBS (■); PBS/silica-1.8 (●); PBS/silica-3.5 (▲).

significant collapse of the network structure between polymer chains and silica was found to occur above critical shear force. Cho and Paul [25] also reported that a decrease in melt viscosity in nylon-6 nanocomposites was related to either the slip between the polymer matrix and the filler material or degradation of the polymer matrix due to high shear heating. However, the rate of decrease in the melt viscosity for PBS/silica composites was not comparable with that of PET/silica composites. This implies that PBS/silica nanocomposites have the potential for enhanced processability in a melt-processing manufacturing system.

TEM images (Fig. 4(a) and (b)) of the fractured surfaces of specimens revealed the aggregation of silica particles dispersed in the PBS matrix. For PBS/silica-3.5, most of the agglomerates were comprised of 10–15 silica particles. In composites formed using fumed silica, significant aggregation of silica particles in the polymer matrix was usually observed below 2 wt% silica due to the high hydrophilicity of fumed silica [23]. Nevertheless, these data indicate that (1) the PBS/silica-3.5 composite approximates the optimum silica content and (2) that the *in situ* polymerization method yields an acceptable distribution of silica throughout the nanocomposite.

The tensile properties of PBS/silica nanocomposites are shown in Table 2. PBS/silica-3.5 exhibited markedly improved tensile properties as compared to parent PBS. For PBS/silica nanocomposites containing more than 3.5 wt% silica, the tensile properties could not be measured as the compressed, molded film was extremely brittle. In the case of PBS/silica-3.5, the stress at break and the strain at break were approximately 39 MPa and 515%, respectively. In general, tensile properties are known to depend largely on the molecular weight of the polymer. However, the combination of WAXD patterns and TEM images obtained in the present study suggest that low crystallinity and silica distribution morphology contribute to significant improvement of tensile properties.

Fig. 5 shows the biodegradability of PBS and PBS/silica nanocomposites. The general expression describing biodegradability is shown in Eq. (1) according to ISO 14853.

Table 2
Tensile properties of PBS and PBS/silica nanocomposites

Sample code	Stress at break (MPa)	Elongation at break (%)	Modulus (MPa)
PBS	26.3(6.9)	96.0(7.3)	331.5(48.5)
PBS/silica-1.8	31.4(4.0)	410.3(27.4)	303.4(14.3)
PBS/silica-3.5	38.6(4.6)	514.5(75.6)	309.5(7.0)
PBS/silica-5.5	–	–	–

Figures in parentheses are standard deviations. Tensile properties of PBS/silica-5.5 could not be measured because compress molded film was extremely brittle.

$$\text{Biodegradation}\% = \frac{\left[\sum(CO_2)_T - \sum(CO_2)_B\right]}{ThCO_2} \times 100 \qquad (1)$$

Here, $\sum(CO_2)_T$ is the amount of CO_2 evolved from the test material between the start of the test and time t, and $\sum(CO_2)_B$ is the amount of CO_2 evolved from the blank test bottle between the start of the test and time t. $ThCO_2$ is the theoretical amount of CO_2 evolved from the test material assuming that all available carbon is transformed into CO_2.

As shown in Fig. 5, the profile of biodegradation, calculated from the accumulated amount of CO_2 evolved, was sigmoidal. In general, low molecular weight materials composed of aliphatic polyesters are subject to biodegradation because of the susceptibility of the aliphatic ester linkage to abiotic hydrolysis [26]. The relative rate of biodegradation observed for the PBS/silica nanocomposites was faster than that of the parent PBS polymer, indicating dependence on silica content. PBS/silica-5.5 nanocomposite films were difficult to prepare for mechanical testing due to their low molecular weight, which should lead to rapid degradation. After 45 days in compost, the rate for biodegradation of PBS/silica-3.5 was approximately 50% faster than that of the parent PBS, which may be attributed to the relatively low crystallinity of the PBS/silica nanocomposites. However, despite the similar degree of crystallinity in both PBS/silica-1.8 and PBS/silica-3.5, the latter showed greater biodegradability. These observations imply that increased amounts of silica result in preferential microbial interactions, leading to the improved biodegradability. Han et al. [27] reported that for

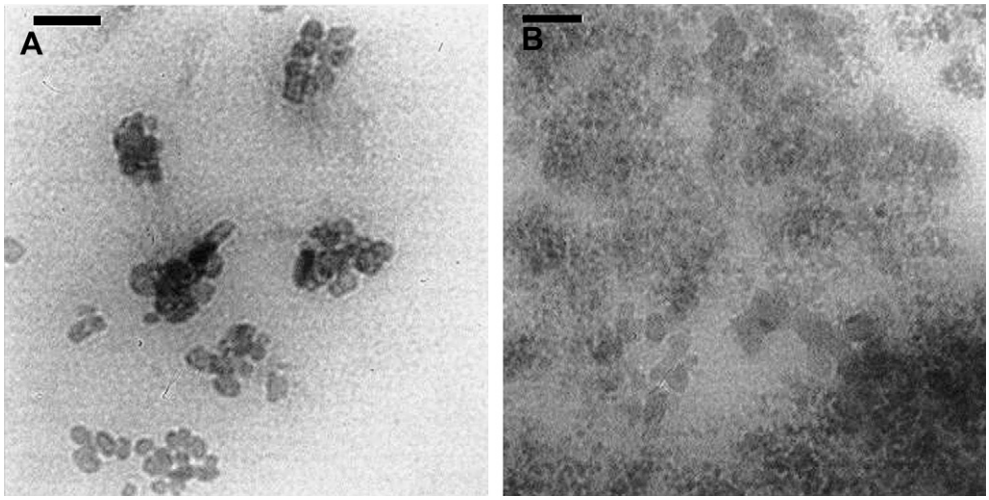

Fig. 4. TEM images of the interfacial area for PBS/silica-3.5 (a) and PBS/silica-5.5 (b). (scale bar: 242 nm).

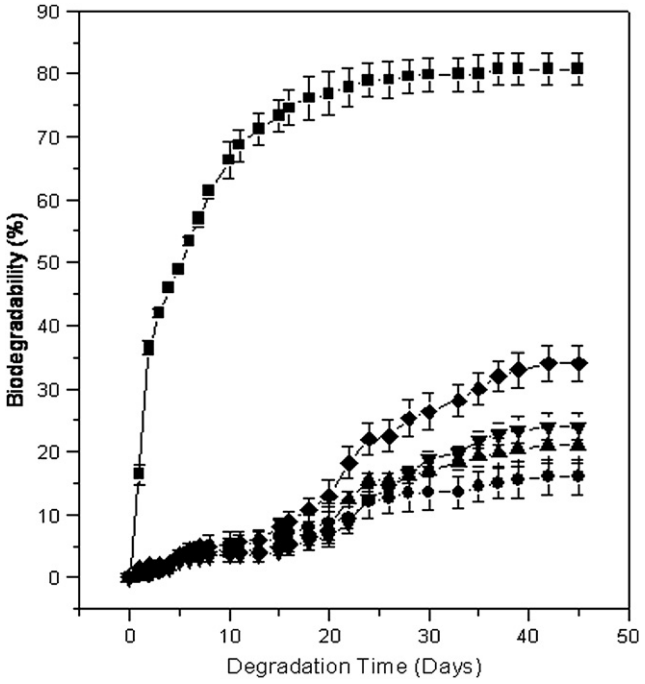

Fig. 5. Biodegradation of PBS/silica nanocomposites in animal fodder compost. Cellulose (■); PBS (●); PBS/silica-1.8 (▲); PBS/silica-3.5 (▼); PBS/silica-5.5 (◆).

aliphatic copolyesters, an increase in hydrophilicity due to free amino groups improved the interactions between the polymer and the degradation enzyme, thereby accelerating degradation. An analogous mechanism may be involved here in which increased hydrophilicity due to the hydroxyl groups on the fumed silica surface may enhance susceptibility to microbial attack.

4. Conclusions

PBS/silica nanocomposites were successfully synthesized in the presence of fumed silica by an *in situ* two-step polymerization method. Solid-state ^{29}Si NMR and FTIR data provided evidence for covalent silanol-bound carbonyl groups. Melt rheological data showed an increased melt viscosity even under high shear force, suggesting that both adequate distribution of silica and the reduced crystallinity are critical factors affecting the physical properties of PBS/silica nanocomposite materials. PBS/silica nanocomposites containing 3.5 wt% of silica had high tensile strength (38.6 MPa) and elongation (515%). The biodegradation rate of the PBS/silica materials was markedly accelerated with increasing silica content. PBS/silica nanocomposites containing 3.5 wt% silica may represent one of the most useful biodegradable materials in terms of acceptable physical properties and enhanced biodegradation rate.

Acknowledgment

This work was supported by the research fund of the Ministry of Commerce, Industry, and Energy of Korea (Grant No. 10014448).

References

[1] Yoo YT, Ko MS, Han SI, Kim TY, Im SS, Kim DK. Degradation and physical properties of aliphatic copolyesters derived from mixed diols. Polym J 1998;30(7):538–45.
[2] Yoo YT, Lee BJ, Han SI, Im SS, Kim DK. Physical properties and biodegradation of poly(butylene adipate) ionomers. Polym Degrad Stab 2003;79(2):257–64.
[3] Han SI, Im SS, Kim DK. Dynamic mechanical and melt rheological properties of sulfonated poly(butylene succinate) ionomers. Polymer 2003;44(23):7165–73.
[4] Han SI, Lee WD, Kim DK, Im SS. Morphology and crystallization behavior of poly(butylene succinate)-based ionomers (PBSi). Macromol Rapid Commun 2004;25(6):753–8.
[5] Han SI, Kang SW, Kim BS, Im SS. A novel polymeric ionomer as a potential biomaterial: crystallization behavior, degradation, and in-vitro cellular interactions. Adv Funct Mater 2005;15(3):367–74.
[6] Han SI, Yoo Y, Kim DK, Im SS. Biodegradable aliphatic polyester ionomers. Macromol Biosci 2004;4(3):199–207.
[7] Park JW, Kim DK, Im SS. Crystallization behaviour of poly(butylene succinate) copolymers. Polym Int 2002;51(3):239–44.
[8] Takiyama E, Fujimaki T. Characteristics of biodegradable aliphatic polymer – bionolle. Plastics 1992;43:87.
[9] Abe H, Doi Y, Hori Y, Hagiwara T. Physical properties and enzymatic degradability of copolymers of (*R*)-3-hydroxybutyric acid and (*S*,*S*)-lactide. Polymer 1998;39(1):59–67.
[10] Tian D, Dubois P, Jerome R. A new poly(epsilon-caprolactone) containing hybrid ceramer prepared by the sol–gel process. Polymer 1996; 37(17):3983–7.
[11] Tian D, Blacher S, Dubois P, Jerome R. Biodegradable and biocompatible inorganic–organic hybrid materials – 2. Dynamic mechanical properties, structure and morphology. Polymer 1998;39(4):855–64.
[12] Ray SS, Maiti P, Okamoto M, Yamada K, Ueda K. New polylactide/layered silicate nanocomposites. 1. Preparation, characterization, and properties. Macromolecules 2002;35(8):3104–10.
[13] Kim HS, Chen GX, Jin HJ, Yoon JS. In situ copolymerization of butylene succinate with twice functionalized organoclay: thermal stability. Colloids Surf A 2008;313–314:56–9.
[14] Lim JS, Noda I, Im SS. Effect of hydrogen bonding on the crystallization behavior of poly 3-hydroxybutyrate-*co*-3-hydroxyhexanoate)/silica hybrid composites. Polymer 2007;48(9):2745–54.
[15] Peeters MPJ, Wakelkamp WJJ, Kentgens APM. A Si-29 solid-state magic-angle-spinning nuclear-magnetic-resonance study of Teos-based hybrid materials. J Non-Cryst Solids 1995;189(1–2):77–89.
[16] Babonneau F, Thorne K, Mackenzie JD. Dimethyldiethoxysilane/tetraethoxysilane copolymers: precursors for the Si–C–O system. Chem Mater 1989;1(5):554–8.
[17] Alam TM, Assink RA, Loy DA. Hydrolysis and esterification in organically modified alkoxysilanes: a Si-29 NMR investigation of methyltrimethoxysilane. Chem Mater 1996;8(9):2366–74.
[18] Young SK, Jarrett WL, Mauritz KA. Nafion (R)/ORMOSIL nanocomposites via polymer-in situ sol–gel reactions. 1. Probe of ORMOSIL phase nanostructures by Si-29 solid-state NMR spectroscopy. Polymer 2002;43(8):2311–20.
[19] Lim JS, Noda I, Im SS. Miscibility and crystallization behavior of poly(3-hydroxybutyrate-*co*-3-hydroxyhexanoate) and methoxy poly(ethylene glycol) blends. J Polym Sci Part B Polym Phys 2006;44(19): 2852–63.
[20] Woo EM, Chiang CP. Glass transition behavior and miscibility in blends of poly(vinyl *p*-phenol) with two homologous aliphatic polyesters. Polymer 2004;45(25):8415–24.
[21] Chen Y, Zhou S, Yang H, Wu L. Structure and properties of polyurethane/nanosilica composites. J Appl Polym Sci 2005;95(5): 1032–9.
[22] Lim JS, Hong SM, Kim DK, Im SS. Effect of isocyanate-modified fumed silica on the properties of poly(butylene succinate) nanocomposites. J Appl Polym Sci 2008;107(6):3598–608.

[23] Hahm WG, Myung HS, Im SS. Preparation and properties of in situ polymerized poly(ethylene terephthalate)/fumed silica nanocomposites. Macromol Res 2004;12(1):85–93.
[24] Chung SC, Hahm WG, Im SS, Oh SG. Poly(ethylene terephthalate) (PET) nanocomposites filled with fumed silicas by melt compounding. Macromol Res 2002;10(4):221–9.
[25] Cho JW, Paul DR. Nylon 6 nanocomposites by melt compounding. Polymer 2001;42(3):1083–94.
[26] Yang HS, Yoon JS, Kim MN. Dependence of biodegradability of plastics in compost on the shape of specimens. Polym Degrad Stab 2005;87(1): 131–5.
[27] Han SI, Kim BS, Kang SW, Shirai H, Im SS. Cellular interactions and degradation of aliphatic poly(ester amide)s derived from glycine and/or 4-amino butyric acid. Biomaterials 2003;24(20): 3453–62.